Radiological Dose Calculations for the Particle Beam Fusion Accelerator Upgrade (PBFA-U)

H.Y. Khater and M.E. Sawan

June 1994

UWFDM-965

Presented at the 3rd International Symposium on Fusion Nuclear Technology, June 26 – July 1, 1994, Los Angeles CA; to be published in *Fusion Engineering and Design*.

FUSION TECHNOLOGY INSTITUTE

UNIVERSITY OF WISCONSIN

MADISON WISCONSIN

Radiological Dose Calculations for the Particle Beam Fusion Accelerator Upgrade (PBFA-U)

H.Y. Khater and M.E. Sawan

Fusion Technology Institute
University of Wisconsin
1500 Engineering Drive
Madison, WI 53706

http://fti.neep.wisc.edu

June 1994

UWFDM-965

Presented at the 3rd International Symposium on Fusion Nuclear Technology, June 26 – July 1, 1994, Los Angeles CA; to be published in *Fusion Engineering and Design*.

Abstract

Biological dose rate calculations are performed for different locations in the vicinity of the target chamber and diode of the PBFA-U facility. The facility is to be used for performing research on light ion beam driven inertial confinement fusion. Depending on the type of diagnostic shots, Bremsstrahlung radiation as well as neutrons are produced. Upon interacting with the diode material, the Bremsstrahlung radiation results in emitting photoneutrons. Results of the activation analysis show that photoneutron production has negligible contribution to the dose rate at the outer casing of the diode following fusion shots. The dose rates are dominated by the contribution from fusion neutrons streaming into the diode. The dose rate in the vicinity of the diode following non-fusion shots is minimal allowing it to be accessed immediately for hands-on maintenance. On the other hand, several shifts of maintenance personnel are required if the outer casing of the diode needs to be accessed following fusion shots to minimize individual exposure. Using steel as structural material for the chamber and diode casing results in lower dose rates compared to aluminum for up to several months following fusion shots. Using steel, the chamber and diode can be accessed 1 day after shots for a maximum of 15 minutes per maintenance shift. Using the aluminum alloy would delay hands-on maintenance to several days following shots.

1. Introduction

PBFA-U is a proposed upgraded version of the Particle Beam Fusion Accelerator (PBFA-II) facility [1] currently operating at Sandia National Laboratory. PBFA-U is an ignition facility which is to be used for performing research on light ion beam driven inertial confinement fusion. The facility will explode targets inside a 1 m radius chamber. Targets at the center of the chamber are imploded by energetic light ions (4.5 MJ). The new facility is expected to operate for 10 years during which three different types of experiments are proposed: beam diagnostic, gas-filled, and cryogenic target implosion. Beam diagnostic shots are expected during the first 5 years of operation at a rate of 500 shots/year. No neutrons are produced during these shots. However, each shot generates 320 kJ of Bremsstrahlung radiation which is produced by energetic electrons in the diode region. Shots on the gas-filled targets during the following 3 years of operation would result in a fusion neutron yield of 10 kJ per shot. The proposed operation schedule for the gas-filled targets also assumes 500 shots/year. Shots on the cryogenic targets (fusion shots) are performed during the final 2 years of operation at a rate of 250 shots/year. Each shot would result in a fusion neutron yield of 10 MJ. Similar to the beam diagnostic shots, shots on gas-filled and cryogenic targets result in a production of 320 kJ of Bremsstrahlung radiation. γ-rays from the Bremsstrahlung radiation result in emitting photoneutrons from the diode structure.

Two-dimensional calculations are performed to calculate the dose rates resulting from the activation by fusion neutrons as well as by photoneutrons generated in the diode. Two different materials are analyzed for use in both the chamber wall and outer casing of the diode: the ferritic steel 2 1/4 Cr-1 Mo and the Al-6061-T6 alloys. The chamber wall thickness differed with the different materials used. A chamber wall made of ferritic steel or aluminum had a thickness of 2 or 4 cm, respectively. A thinner steel wall is used because of the relatively good fatigue life characteristics of the 2 1/4 Cr-1 Mo steel. The inner surface of the chamber wall is protected by a 1 cm thick graphite (H-451) liner. The chamber is surrounded by a 3 meter thick water tank for neutron shielding. The possibilities of achieving better neutron shielding by replacing the water in the tank with borated water and adding a 1 cm thick sheet of boral (a B_4C-Al mixture) on the outer

surface of the wall are also assessed. The borated water contains boric acid (H_3BO_3) at a concentration of 5 g/100 cm^3. The primary diode material considered in this analysis is the Ti-6Al-4V alloy. Results of the activation analyses are used to calculate the biological dose rates at the back of the water tank, at the anode and at the outer casing of the diode.

2. Neutron Transport Calculations

Two-dimensional coupled neutron-gamma transport calculations are performed using the two-dimensional discrete ordinates neutron transport code TWODANT [2] with ENDF/B-V cross section data. The analysis uses a P_3 approximation for the scattering cross sections and S_8 angular quadrature set. An inherent problem associated with multi-dimensional discrete ordinates calculations with localized sources is referred to as the "ray effect". It is related to the fact that the angular flux is given only in certain discrete directions. It is, therefore, not possible to exactly represent the component in the normal direction ($\mu = 1$) along the beam penetration which can lead to underestimating neutron streaming. We have fully mitigated the ray effect by using the first collision method [3]. In this method, the uncollided flux is determined analytically and the volumetrically distributed first collision source is used in the calculations.

The problem has been modeled in spherical geometry with a point source at the center of the chamber. An R-Z geometry is utilized with the target represented by an isotropic point source on the Z-axis. Figure 1 shows the two-dimensional model used in the calculations. The source emits neutrons and gamma photons with energy spectra determined from target neutronics calculations for a generic single shell target [4]. 3.55×10^{15} and 3.55×10^{18} (14.1 MeV) D-T neutrons are produced by the 10 kJ and 10 MJ fusion shots, respectively. In the same time, about 5.28×10^{12} photoneutrons are estimated to be produced per shot. Figures 2 and 3 show the prompt dose (for the 10 MJ shots) as a function of distance from the diode (Z-direction) during operation for the two cases, without or with the three meter water tank in place, respectively. Without water shield, the prompt dose is dominated by neutron scattering and gamma production in the diode outer casing. On the other hand, with the water shield in place, the prompt dose is dominated by interactions of the streaming neutrons with the coil materials resulting in the two humps shown in Fig. 3. The

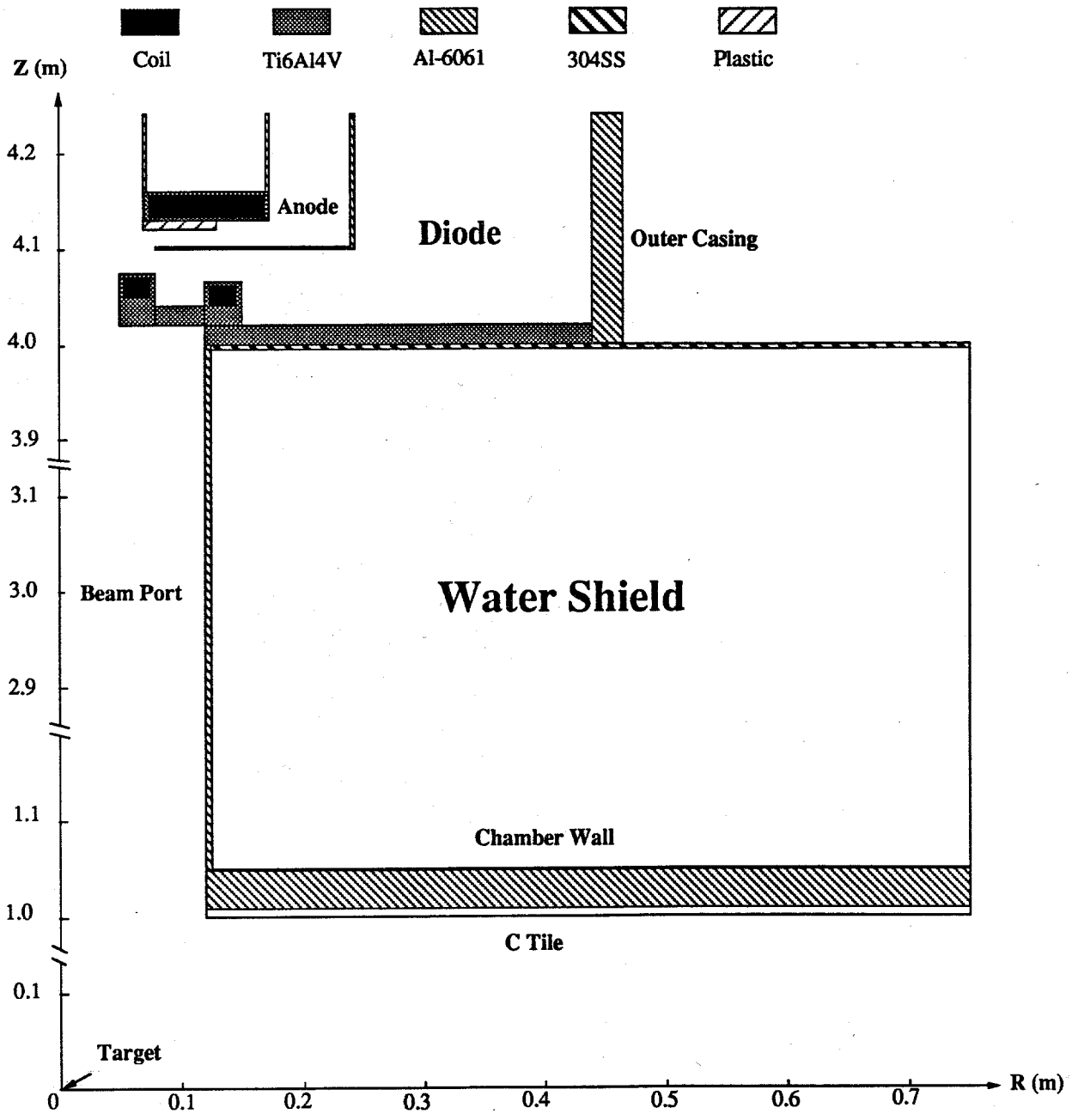

Fig. 1. Two-dimensional model for the chamber and diode.

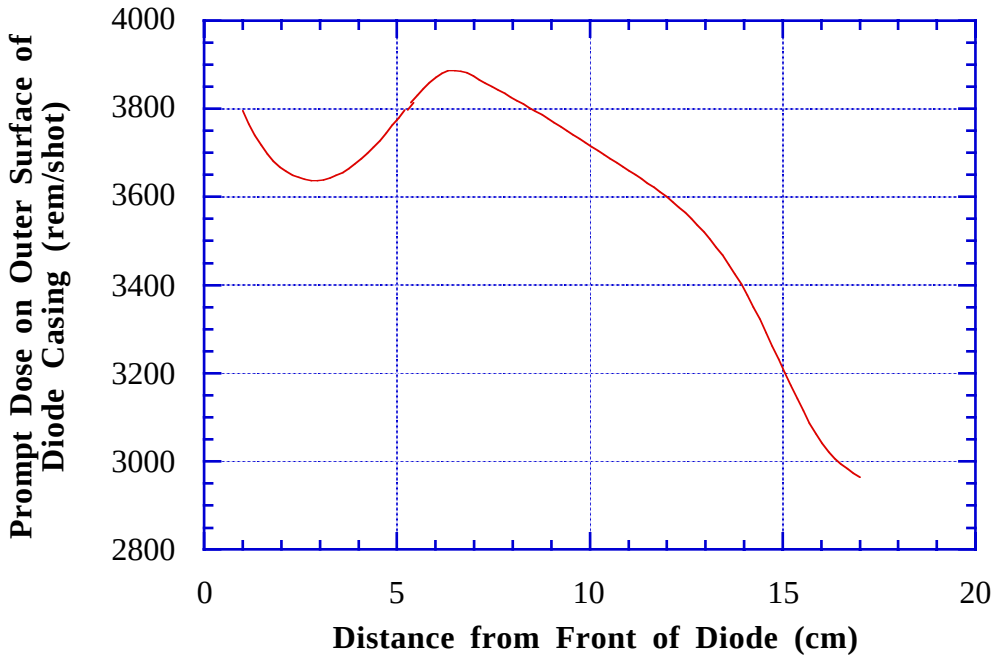

Fig. 2. Prompt dose around the diode during operation with no water tank in place.

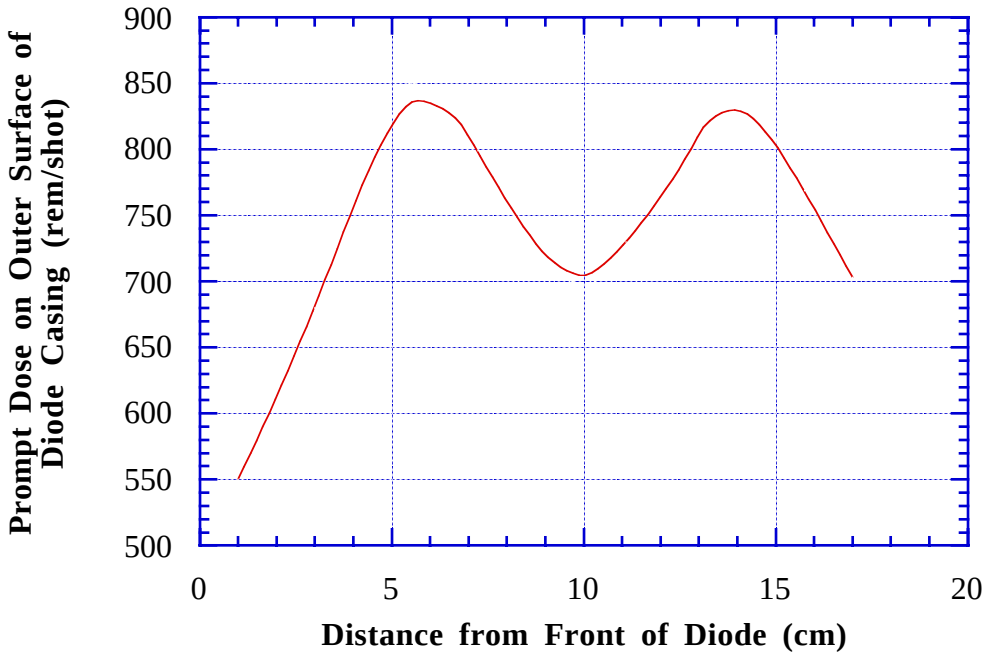

Fig. 3. Prompt dose around the diode during operation with water tank in place.

presence of the water tank reduces the operational dose by a factor of five or more. As shown in the figures, the doses which are mostly caused by the fusion neutrons streaming into the diode are too high. Therefore, no access to the area near the diode should be allowed during shots.

3. Activation Analysis

The neutron flux obtained from the neutron transport calculations is used in the activation calculations. The calculations are performed using the computer code DKR-ICF [5] with the ACTL [6] activation cross section library. The neutron transmutation data used is in a 46 group structure format. The decay and gamma source data are taken from the table of isotopes [7] with the gamma source data being in 21 group structure format. The calculations are performed assuming ten years of operation. Using the DKR-ICF code allows for appropriate modeling of the pulse sequence in ICF chambers. In a previous analysis of the Laboratory Microfusion Facility [8], it was shown that assuming an equivalent steady state operation (where the flux level is reduced to conserve fluence) results in underestimating the dose rates at shutdown by several orders of magnitude. The underestimation becomes negligible within a week from shutdown. The large underestimation within a short period of time following shutdown is due to the fact that the activity during this time is dominated by short-lived radionuclides. The activities of short-lived isotopes are usually sensitive to the operational schedule prior to shutdown due to its buildup during the on-time with subsequent decay during the dwell time. On the other hand, the long term activity is dominated by long-lived radionuclides whose activity is determined by the total neutron fluence regardless of the temporal variation of the flux level.

During the first eight years of operation, the calculations assume 500 shots per year. Hence, the pulsing schedule considered here allows for two shots per day which are 6 hours apart with 18 hours between the daily shots. Operating for 5 days a week results in ten shots per week. Therefore, fifty weekly pulse sequences are considered in each year. This scenario allows for 66 hours at the end of each week where no shots take place. The pulsing sequence during the last two years of operation is based on assuming 250 shots per year. The calculation used a pulse per day during 5 days of each week with no operation during the last 2 days of the week. Shots are only

assumed during the first 50 weeks and no shots are considered during the last 2 weeks of each year. As mentioned before, while no neutrons are produced during the first five years, low-yield neutrons (10 kJ) are produced in the following 3 years. High-yield neutrons (10 MJ) are included in the calculation of the last 2 years. Photoneutrons from the Bremsstrahlung radiation are considered during each of the 10 years of operation.

The decay gamma source produced by the DKR-ICF code is used to calculate the biological dose rate after shutdown using the DOSE [5] code. The DKR-ICF code gives the decay gamma source at different times following shutdown. The adjoint dose field is then determined by performing a gamma adjoint calculation using the TWODANT code with the flux-to-dose conversion factors representing the source at the point where the dose is calculated. The decay gamma source and the adjoint dose field are then combined to determine the biological dose rate at different times following shutdown.

4. Dose Rates Near the Diode

Neutrons streaming through the beam ports and into the diode region dominate the dose values produced in the vicinity of the diode. In the same time, much smaller levels of dose are caused by the photoneutrons produced as a result of the interaction between the Bremsstrahlung radiation and the diode materials. As shown in Table 1, if aluminum is used in the chamber wall and diode casing, the dose rates near the diode are higher than their values if the ferritic steel alloy is used. After one day following shutdown, using aluminum results in twice the dose with steel. Only at one year following shutdown the dose using steel is higher due to the decay of ^{54}Mn and ^{60}Co. If diodes need to be serviced following each shot, and based on a maximum allowable dose limit of 0.5 rem/year, the maximum dose rate allowable for a worker participating in all shifts is limited to 2 mrem per shift. Therefore, using steel, the chamber and diode can be accessed 1 day after shots for a maximum of 15 minutes per maintenance shift. Using the aluminum alloy would delay hands-on maintenance to several days following shots. As shown in Table 2, using the aluminum alloy, the dose near the anode is a factor of four to five higher than the dose near the

Table 1

Dose Rates Near the Diode (mrem/hr)

Time Following Shutdown	2 1/4 Cr-1 Mo	Al-6061-T6
At shutdown	4.64×10^{4}	6.61×10^{4}
1 min	7.75×10^{2}	2.02×10^{3}
10 min	2.86×10^{2}	8.05×10^{2}
1 hr	31.4	54.66
6 hr	13.7	25.56
1 day	7.47	15.6
1 week	2.3	3.71
1 month	1.58	2.36
1 year	0.33	0.28
10 years	1.25×10^{-2}	2.02×10^{-2}
100 years	8.17×10^{-7}	2.74×10^{-6}
1000 years	7.26×10^{-7}	2.59×10^{-6}

Table 2

Dose Rates at Different Locations in the Vicinity of the Diode (mrem/hr)

Time Following Shutdown	Near the Anode	Near the Outer Casing
At shutdown	2.22×10^{5}	6.61×10^{4}
1 min	8.92×10^{3}	2.02×10^{3}
10 min	3.83×10^{3}	8.05×10^{2}
1 hr	2.52×10^{2}	54.66
6 hr	1.03×10^{2}	25.56
1 day	62.6	15.6
1 week	18.4	3.71
1 month	12.2	2.36
1 year	1.69	0.28
10 years	0.12	2.02×10^{-2}
100 years	9.74×10^{-6}	2.74×10^{-6}
1000 years	8.84×10^{-6}	2.59×10^{-6}

outer casing. Hence, access to the area near the anode should be limited to remote maintenance during the first week following shots.

In the case with aluminum alloy in the chamber wall and outer casing of the diode, the dose rates within the first few minutes following the facility shutdown are dominated by the decay of ^{26}Na ($T_{1/2}$ = 1.07 s) produced from ^{26}Mg through an (n,p) reaction. During the first few hours, the doses are dominated by ^{27}Mg ($T_{1/2}$ = 9.45 min) produced from ^{26}Mg (n,γ), ^{27}Al (n,p), and ^{30}Si (n,α), ^{28}Al ($T_{1/2}$ = 2.25 min) produced from ^{27}Al (n,γ) and ^{28}Si (n,p), and ^{24}Na ($T_{1/2}$ = 14.96 hr) produced from ^{23}Na (n,γ), ^{24}Mg (n,p), and ^{27}Al (n,α) reactions. The dose rates during the first week continue to be dominated by the decay of ^{24}Na. ^{54}Mn ($T_{1/2}$ = 312.2 d) and ^{60}Co ($T_{1/2}$ = 5.271 yr) are the dominant nuclides in the period up to ten years following shutdown. While ^{54}Mn is produced from both ^{54}Fe (n,p) and ^{55}Mn (n,2n) reactions, ^{60}Co is mostly produced from the ^{60}Ni (n,p) reaction. At times beyond 10 years after shutdown, the dose rates are caused by the decay of the ^{26}Al ($T_{1/2} = 7.3 \times 10^5$ yr). ^{26}Al is produced via the ^{27}Al (n,2n) reaction. All of the dominant radionuclides, except ^{60}Co, are produced from magnesium, aluminum, silicon, and manganese which are constituent elements of the Al-60661-T6 alloy. On the other hand, the radionuclide ^{60}Co is produced from the impurity element nickel. Nickel is a trace element in both iron (60 wppm) and chromium (3 wppm). Iron and chromium are also constituent elements of Al-6061-T6.

In the case of the 2 1/4 Cr-1 Mo steel chamber, the dose rate during the first few minutes following shutdown is dominated by ^{28}Al and ^{52}V ($T_{1/2}$ = 3.76 min) produced from ^{51}V (n,γ), ^{52}Cr (n,p), and ^{55}Mn (n,α) reactions. The high content of manganese in the steel chamber results in ^{56}Mn ($T_{1/2}$ = 2.578 hr) being the major contributor to the dose rate up to one day. Even though most of the ^{56}Mn is produced as a result of the ^{55}Mn (n,γ) reaction, a significant amount is also produced by the ^{56}Fe (n,p) reaction. In the period between 1 day and 10 years, as in the case of the aluminum chamber, ^{54}Mn and ^{60}Co dominate the dose rate produced in the steel chamber. Beyond ten years after shutdown, the dose rate is primarily dominated by radionuclides induced from the steel impurities. The two major contributors are ^{94}Nb ($T_{1/2} = 2 \times 10^4$ yr) produced from

^{93}Nb (n,γ) and ^{94}Mo (n,p), and ^{93}Mo ($T_{1/2}$ = 3,500 yr) produced from ^{92}Mo (n,γ) and ^{94}Mo (n,2n) reactions.

Since PBFA-U has twenty diodes and the total Bremsstrahlung yield per shot is 320 kJ, the resulting Bremsstrahlung yield per diode per shot is 16 kJ. The Bremsstrahlung spectrum has an end point at 20 MeV and a peak value at 0.1 MeV. The average photon energy is about 1.9 MeV, resulting in a photon yield per shot per diode of 5.3×10^{16} photons. Only 2.3% of these photons carry energies in excess of 10 MeV. Using experimental cross section data for the Ti (γ,n) reaction, the photoneutron production in the diode region is estimated at 5.28×10^{12} neutrons per shot. The calculated photoneutron source is utilized in a two-dimensional analysis to calculate the photoneutron-induced doses at different locations near the diode. The peak operational dose (prompt) dose at the outer casing of the diode resulting from photoneutrons is 12 rem/shot. In addition, the delayed dose rates caused by the activation of the diode materials is calculated for the Al-6061-T6 option. As shown in Table 3, the highest dose is produced at the location nearest to the anode. On the other hand, photoneutrons produce their lowest dose level near the outer casing of the diode. The doses due to the photoneutrons are quite small such that using either the aluminum or ferritic steel alloys in the outer casing of the diode had no effect on the overall dose values.

5. Dose Rates Away from Penetrations

Streaming neutrons have a minimal effect on the dose rates found at the back of the water tank and away from the penetrations. In this case, most of the dose is produced by neutrons interacting with the chamber wall after undergoing a considerable slowing down while travelling through the water filled tank. At shutdown, the dose is more than an order of magnitude lower than its value near the diode. The dose drops by four orders of magnitude within one hour and six orders of magnitude within the first week following shutdown in comparison to its value near the diode. For the two alloys considered in this paper, the chamber wall can be accessed within 15

Table 3

Dose Rates Produced by Photoneutrons Near the Diode (mrem/hr)

Time Following Shutdown	Near the Anode	Near the Outer Casing
At shutdown	3.06	1.3
1 min	2.66	1.17
10 min	1.11	0.55
1 hr	0.19	3.6×10^{-2}
6 hr	0.15	1.94×10^{-2}
1 day	0.11	1.25×10^{-2}
1 week	3.92×10^{-2}	2.86×10^{-3}
1 month	2.61×10^{-2}	1.77×10^{-3}
1 year	2.97×10^{-3}	1.85×10^{-4}
10 years	8.11×10^{-5}	4.61×10^{-6}
100 years	5.88×10^{-10}	3.34×10^{-11}
1000 years	1.15×10^{-11}	5.99×10^{-13}

minutes from shutdown if one stays far enough from the diode to avoid any direct contact with gamma rays resulting from the decay of radioactive nuclides produced by the streaming neutrons.

A comparison between the contact dose rates for the two alloys considered is shown in Fig. 4. The large amount of ^{24}Na produced in the aluminum chamber results in higher contact dose rates than the steel chamber up to approximately 10 days after shutdown. A significant drop in the aluminum chamber dose rate levels occurs after about one day due to the decay of ^{24}Na. This results in the steel dose being at least about a factor of five higher than the Al-6061-T6 dose over the period between 1 week and 5 years due to its higher content of ^{54}Mn. The aluminum alloy results in a much higher dose than the steel alloys for times exceeding 10 years following shutdown. At these times, ^{26}Al is the sole contributor to the dose. Finally, as shown in Fig. 5, filling the tank with borated water or a combination of a borated water filled tank and a layer of boral placed on the outer surface of the chamber wall, result in reducing the shutdown dose rate by only 60%. The results shown in the figure are for the aluminum alloy case.

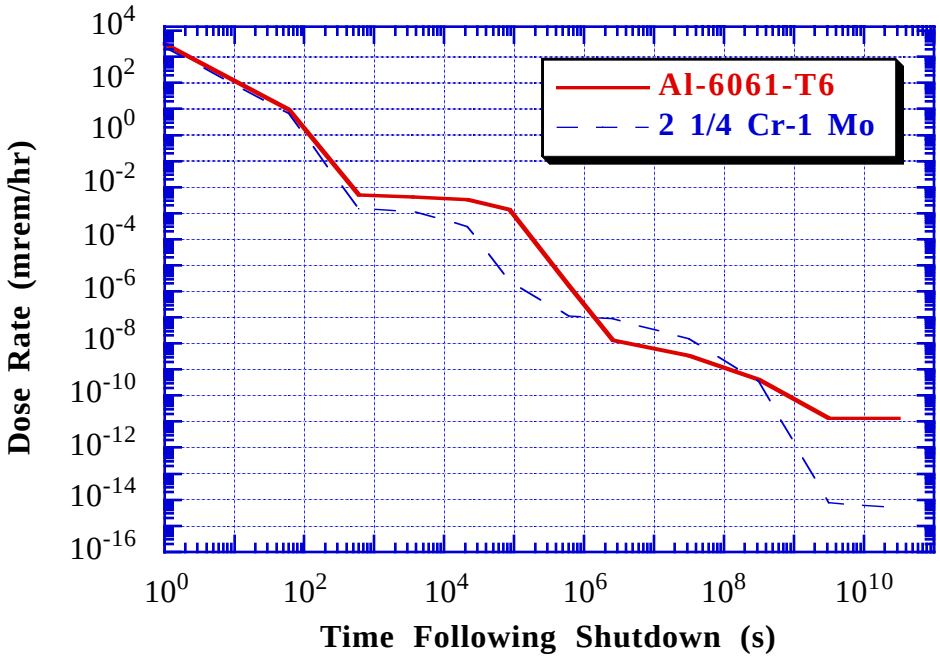

Fig. 4. Comparison between contact dose rates away from the diode.

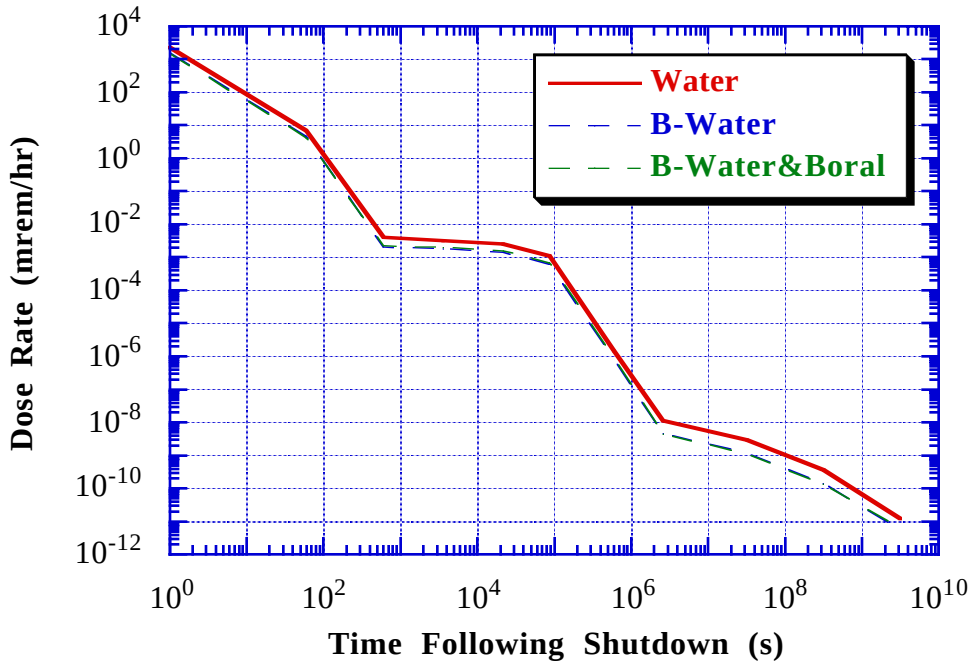

Fig. 5. Impact of using borated water and boral on the contact dose rates away from the diode.

6. Summary

PBFA-U is a proposed upgraded version of the Particle Beam Fusion Accelerator (PBFA-II) facility currently operating at Sandia National Laboratory. Activation analyses are performed for both the target chamber and diode of PBFA-U. Two-dimensional calculations are performed to calculate the dose rates near the diode and away from penetrations. Photoneutrons generated in the diode as well as fusion neutrons streaming into the diode are considered in the analysis. The first collided source method is used in the two-dimensional discrete ordinates calculations to mitigate the ray effect and account for all fusion neutrons streaming into the diode. Ferritic steel 2 1/4 Cr-1 Mo and the Al-6061-T6 alloys are analyzed for use in both the chamber wall and outer casing of the diode. Dose rates are calculated at the back of the water tank, at the anode, and at the outer casing of the diode.

The analysis shows that photoneutron production has negligible contribution to the dose rate at the outer casing of the diode following fusion shots. Fusion neutrons streaming into the diode dominate the overall dose rate. The dose rate in the vicinity of the diode due to photoneutrons produced during non-fusion shots is minimal, allowing it to be accessed immediately for hands-on maintenance. On the other hand, several shifts of maintenance personnel are required if the outer casing of the diode needs to be accessed following fusion shots to minimize individual exposure. Using steel as structural material for the chamber and diode casing results in lower dose rates compared to aluminum for up to several months following fusion shots. Using steel, the chamber and diode can be accessed 1 day after shots for a maximum of 15 minutes per maintenance shift. Using the aluminum alloy would delay hands-on maintenance to several days following shots.

Acknowledgment

Support for this work was provided by Sandia National Laboratory, Albuquerque, New Mexico.

References

[1] B. N. Turman et al., "PBFA-II, A 100 TW Pulsed Power Driver for the Inertial Confinement Fusion Program," Digest of Technical Papers, 5th IEEE Pulsed Power Conference (1986), pp. 155.

[2] R. Alcouffe et al., "User's Guide for TWODANT: A Code Package for Two-Dimensional, Diffusion-Accelerated, Neutral-Particle Transport," Los Alamos National Laboratory, LA-10049-M (March 1984).

[3] R. Alcouffe, R. O'Dell, and F. Brinkley, Jr., "A First-Collision Source Method that Satisfies Discrete S_n Transport Balance," *Nuclear Engineering & Design*, **105**, 198 (1990).

[4] D. L. Henderson, M. E. Sawan, and G. A. Moses, "Radiological Dose Calculations for the Diode Region of the Light Ion Fusion Target Development Facility," *Fusion Technology*, **13**, 594 (1988).

[5] D. Henderson and O. Yasar, "DKR-ICF: A Radioactivity and Dose Rate Calculation Code Package," University of Wisconsin, UWFDM-714 (April 1987).

[6] M. A. Gardner and R. J. Howerton, "ACTL: Evaluated Neutron Activation Cross Section Library - Evaluation Techniques and Reaction Index," Lawrence Livermore National Laboratory, UCRL-50400, Vol. 18 (1978).

[7] C. Lederer and V. Shirley, Table of Isotopes, 7th ed., John Wiley & Sons, Inc., New York (1978).

[8] H. Y. Khater and M. E. Sawan, "Dose Rate Calculations for a Light Ion Beam Fusion Laboratory Microfusion Facility," Proc. IEEE Thirteenth Symposium on Fusion Engineering, Knoxville, TN (October 1989), pp. 1412-1415.